

**CONJUGACIES PROVIDED BY FRACTAL TRANSFORMATIONS I :
CONJUGATE MEASURES, HILBERT SPACES, ORTHOGONAL
EXPANSIONS, AND FLOWS, ON SELF-REFERENTIAL SPACES.**

CHRISTOPH BANDT, MICHAEL BARNSELY, MARKUS HEGLAND, AND ANDREW VINCE

ABSTRACT. Theorems and explicit examples are used to show how transformations between self-similar sets (general sense) may be continuous almost everywhere with respect to stationary measures on the sets and may be used to carry well known flows and spectral analysis over from familiar settings to new ones. The focus of this work is on a number of surprising applications including (i) what we call fractal Fourier analysis, in which the graphs of the basis functions are Cantor sets, being discontinuous at a countable dense set of points, yet have very good approximation properties; (ii) Lebesgue measure-preserving flows, on polygonal laminas, whose wave-fronts are fractals. The key idea is to exploit fractal transformations to provide unitary transformations between Hilbert spaces defined on attractors of iterated function systems. Some of the examples relate to work of Oxtoby and Ulam concerning ergodic flows on regions bounded by polygons.

1. INTRODUCTION

In this paper we provide results and explicit examples to show how transformations between some fractals, and other self-referential sets, may both be continuous almost everywhere and map well-known flows and spectral analysis from familiar settings to new ones. Our focus is on a number of surprising applications including: (i) what we call "fractal Fourier analysis", in which the basis functions are discontinuous at a countable dense set of points of a real interval, yet have good approximation properties; (ii) Lebesgue measure-preserving flows on tori whose wave-fronts are fractal curves.

The key idea is to exploit fractal transformations to provide unitary transformations between Hilbert spaces defined on attractors of iterated function systems. Some of our examples relate to the work of Oxtoby and Ulam [22], concerning ergodic flows on real geometrical domains.

Let A_F and A_G be non-overlapping attractors of two contractive iterated function systems (IFSs), F and G respectively. We give conditions under which the fractal transformation $T_{FG} : A_F \rightarrow A_G$ (defined in Section 2) is measurable and continuous almost everywhere with respect to any stationary measure μ_F (defined in Section 2). We show that T_{FG} yields an isometry $U_{FG} : \mathcal{L}^2(A_F, \mu_F) \rightarrow \mathcal{L}^2(A_G, \mu_G)$, where μ_F and μ_G are a corresponding pair of stationary measures. If $L_F : D_F \subset \mathcal{L}^2(A_F, \mu_F) \rightarrow \mathcal{L}^2(A_F, \mu_F)$ is a linear operator with dense domain D_F , then

$$L_G := U_{FG} L_F U_{GF}$$

is a linear operator on $\mathcal{L}^2(A_G, \mu_G)$ with dense domain $T_{FG}(D_F)$. If L_F is self-adjoint, then so is L_G . In some cases μ_F is Lebesgue measure on a subset of \mathbb{R}^n such as line segment, a filled triangle, or a cube; and in other cases it is a uniform measure on a fractal such as a Sierpinski triangle. In these cases, familiar differential and integral equations, including those associated with Laplacians on post critically finite (p.c.f.) fractals [19, 28], can be transformed to yield interesting counterparts on other (not necessarily p.c.f.) fractals.

By way of examples (i) we introduce what we call "fractal Fourier analysis", in which the basis functions are discontinuous at a countable dense set of points, yet have good approximation properties including overcoming the edge-effect problem that besets standard Fourier approximation; and (ii) we introduce and exemplify certain flows on self-similar sets, we provide rough versions of flows on tori, and we exhibit the solution of a heat equation on a rough filled triangle, with Dirichlet boundary conditions.

2. FRACTAL TRANSFORMATIONS AND INVARIANT MEASURES

This section introduces some essential concepts that run throughout the paper, including the invariant measure of an IFS with probabilities, called a p -measure, and fractal transformations from the attractor of one IFS to the attractor of another. The main result of this section are Theorem 2.1 which states that if an attractor is not equal to its dynamical boundary, then all p -measures of the critical set, the dynamical boundary, and the forward orbit of overlap set under the IFS (which we call the inner boundary), are zero; and Theorem 2.3 which states that a fractal transformation between non-overlapping attractors is measurable and continuous almost everywhere with respect to every p -measure, and that a such a fractal transformation is p -measure preserving.

2.1. Non-Overlapping Attractors and Fractal Transformations. The purpose of this subsection is to define the central notions of non-overlapping attractor and fractal transformation from one attractor to another.

Let $\mathbb{N} = \{1, 2, 3, \dots\}$ and $\mathbb{N}_0 = \{0, 1, 2, \dots\}$. Throughout this paper we restrict attention to iterated function systems (IFSs) of the form

$$F = \{X; f_1, f_2, \dots, f_N\}$$

where $N \in \mathbb{N}$ is fixed, X is a complete metric space, and $f_i : X \rightarrow X$ is a contraction for all $i \in I := \{1, 2, \dots, N\}$. By **contraction** we mean there is $\lambda \in [0, 1)$, such that $d_{\mathbb{X}}(f_i(x), f_i(y)) \leq \lambda d_{\mathbb{X}}(x, y)$ for all $x, y \in X$, for all $i \in I$.

Define $F^{-1} : 2^A \rightarrow 2^A$ and $F : 2^A \rightarrow 2^A$ by

$$F^{-1}(U) = \cup_{i=1}^N f_i^{-1}(U) \text{ and } F(U) = \cup_{i=1}^N f_i(U),$$

for all $U \subset A$, where $f_i^{-1}(U) = \{x \in A : f_i(x) \in U\}$, and $f_i(U) = \{f_i(x) \in A : x \in U\}$. Let F^{-k} mean F^{-1} composed with itself k times, let F^k mean F composed with itself k times, for all $k \in \mathbb{N}$, and let $F^0 = F^{-0} = I$.

If $\mathbb{H}(X)$ denotes the collection of nonempty compact subsets of X , then the classical Hutchinson operator $F : \mathbb{H}(X) \rightarrow \mathbb{H}(X)$ is just the operator F above restricted to $\mathbb{H}(X)$. According to the basic theory of contractive IFSs as developed in [17], there is unique **attractor** $A \subset X$ of F . That is, A is the unique nonempty compact subset of X such that

$$A = F(A).$$

The attractor A has the property

$$A = \lim_{k \rightarrow \infty} F^k(S),$$

where convergence is with respect to the Hausdorff metric and is independent of $S \in \mathbb{H}(X)$.

Since, in this paper, we are only interested in A itself, henceforth let $X = A$. Moreover, throughout this paper the following assumptions are made:

- $F = \{A; f_1, f_2, \dots, f_N\}$ is an IFS with attractor A and such that each of its functions is a contraction and is a homeomorphism onto its image.

(Note that, under these assumptions, $f_i^{-1}(S) := \{a \in A : f_i(a) \in S\} = f_i^{-1}(f_i(A) \cap S)$ for all i , for all $S \subset A$.)

Let $I = \{1, 2, \dots, N\}$, and let I^∞ , referred to as the **code space**, be the set of all infinite sequences $\theta = \theta_1\theta_2\theta_3 \dots$ with elements from I . The **shift operator** $S : I^\infty \rightarrow I^\infty$ is defined by $S(\theta_1\theta_2\theta_3 \dots) = \theta_2\theta_3\theta_4 \dots$. Define a metric d on $I^\infty = \{1, 2, \dots, N\}^\infty$ so that, for $\theta, \sigma \in I^\infty$ with $\theta \neq \sigma$, the distance $d(\theta, \sigma) = 2^{-k}$, where k is the least integer such that $\sigma_k \neq \theta_k$. The pair (I^∞, d) is a compact metric space.

Definition 2.1. The **coding map**, $\pi : I^\infty \rightarrow A$ is defined by

$$\pi(\sigma) = \lim_{k \rightarrow \infty} f_{\sigma_1} \circ f_{\sigma_2} \circ \dots \circ f_{\sigma_k}(a),$$

for any fixed $a \in A$, for all $\sigma = \sigma_1\sigma_2 \dots \in I^\infty$.

Under the assumption that the IFS is contractive, it is well known that the limit is a single point, independent of $a \in A$, convergence is uniform over I^∞ , and π is continuous and onto.

Example 2.1 (The code space IFS). The IFS $Z = \{I^\infty; s_1, s_2, \dots, s_N\}$, where $s_i : I^\infty \rightarrow I^\infty$ is defined by $s_i(\sigma) = i\sigma$, satisfies all the conditions. In particular, the contraction constant for all i is $\lambda = \frac{1}{2}$. In this case π is the identity map on I^∞ .

Definition 2.2. Define the **critical set** of A (w.r.t. F) to be

$$C = \bigcup_{i \neq j} f_i(A) \cap f_j(A).$$

Let \bar{U} be the closure of $U \subset A$.

Definition 2.3. Define the **dynamical boundary** of A (w.r.t. F) to be

$$\partial A = \overline{\bigcup_{k=1}^{\infty} F^{-k}(C)}.$$

The notion of the dynamical boundary was introduced by Morán [20], in the context of similitudes on \mathbb{R}^n . In general, ∂A is not equal to the topological boundary of A (see Example 2.2).

Definition 2.4. For the IFS F , we define the **inner boundary** of the attractor A (w.r.t. F) to be

$$\hat{C} = \bigcup_{k \in \mathbb{N}_0} F^k(C).$$

The inner boundary of A is the set of points with more than one address: a proof of the following proposition appears in [18].

Proposition 2.1. $\hat{C} = \{x : |\pi^{-1}(x)| \neq 1\}$.

Definition 2.5. Define A_F to be **non-overlapping** (w.r.t. F) when

$$A \neq \partial A.$$

Example 2.2. Let $F = \{[0, 1]; f_1, f_2\}$, where the metric on the unit interval $[0, 1]$ is the Euclidean metric. Note that the topological boundary of $[0, 1]$ is empty; every point in $[0, 1]$ lies in its interior. If $f_1(x) = \frac{1}{2}x$, $f_2(x) = \frac{1}{2}x + \frac{1}{2}$, then the dynamical boundary of the attractor $A = [0, 1]$ is $\partial A = \{0, 1\}$. In this case, by definition, A is non-overlapping. On the other hand, if $f_1(x) = \frac{2}{3}x$, $f_2(x) = \frac{2}{3}x + \frac{1}{3}$, then again $A = [0, 1]$, but $\partial A = [0, 1]$. In this case A is overlapping.

We are going to need the following topological lemma, which generalizes a result in [13]. A point $\omega \in I^\infty$ is called **disjunctive** if $\{S^k\omega : k \in \mathbb{N}\}$ is dense in I^∞ .

Lemma 2.1. *Let $F = \{A; f_1, f_2, \dots, f_N\}$ be an IFS with attractor A , and let $\omega \in I^\infty$ be disjunctive. We have $\pi(\omega) \in A \setminus \partial A$ if and only if $A \setminus \partial A \neq \emptyset$.*

Proof. We begin with two observations. (i) The set ∂A is closed and $F^{-1}(\partial A) \subset \partial A$. Hence, if $\theta \in I^\infty$ obeys $\pi(\theta) \in \partial A$, then $\pi(S\theta) \in \partial A$, whence $\pi(S^k\theta) \in \partial A$ for all $k \in \mathbb{N}_0$, whence $\overline{\{\pi(S^k\theta)\}_{k=0}^{\infty}} \subset \partial A$. (ii) If $\omega \in I^\infty$ is disjunctive, then, using the continuity of π , $\overline{\{\pi(S^k\omega)\}_{k=0}^{\infty}} = A$.

Let $\omega \in I^\infty$ be disjunctive.

(\Rightarrow) Suppose that $\pi(\omega) \in A \setminus \partial A$. Then $A \setminus \partial A \neq \emptyset$.

(\Leftarrow) Suppose that $A \setminus \partial A \neq \emptyset$. If $\pi(\omega) \in \partial A$, it follows that $S^k\omega \in \partial A$ for all k , so by (i) and (ii), $A = \overline{\{\pi(S^k\omega)\}_{k=0}^{\infty}} \subset \partial A$; but $\partial A \subset A$, so $A = \partial A$; hence $A \setminus \partial A = \emptyset$, which is not possible, so $\pi(\omega) \in A \setminus \partial A$. \square

The code space I^∞ is equipped with the lexicographical ordering, so that $\theta > \sigma$ means $\theta \neq \sigma$ and $\theta_k > \sigma_k$ where k is the least index such that $\theta_k \neq \sigma_k$. Here $1 > 2 > 3 \dots > N - 1 > N$.

Definition 2.6. A **section** of the coding map $\pi : I^\infty \rightarrow A$ is a map $\tau : A \rightarrow I^\infty$ such that $\pi \circ \tau$ is the identity. In other words τ is a map that assigns to each point in A an *address* in the code space. The **top section** of $\pi : I^\infty \rightarrow A$ is the map $\tau : A \rightarrow I^\infty$ given by

$$\tau(x) = \max \pi^{-1}(x)$$

for all $x \in A$, where the maximum is with respect to the lexicographic ordering. The value $\tau(x)$ is well-defined because $\pi^{-1}(x)$ is a closed subset of I^∞ .

The top section is forward shift invariant in the sense that $S(\tau(A)) = \tau(A)$. See [9] for a classification, in terms of masks, of all shift invariant sections, namely sections such that $S(\tau(A)) \subset \tau(A)$.

Definition 2.7. Let A_F and A_G be the attractors, respectively, of IFSs $F = \{A_F; f_1, f_2, \dots, f_N\}$ and $G = \{A_G; g_1, g_2, \dots, g_N\}$ with the same number of functions. The **fractal transformations** $T_{FG} : A_F \rightarrow A_G$ and $T_{GF} : A_G \rightarrow A_F$ are defined (see for example [4, 8]) to be

$$T_{FG} = \pi_G \circ \tau_F \quad \text{and} \quad T_{GF} = \pi_F \circ \tau_G,$$

where τ is the top section. If T_{FG} is a homeomorphism, then it is called a **fractal homeomorphism**, and in this case $T_{GF} = (T_{FG})^{-1}$.

A more general notion of fractal transformation is similarly defined by taking τ to be any shift invariant section; see [9]. The following simple proposition is useful. It is well-known, see for example [6, Theorem 1] and [8], for references and subtler results.

Proposition 2.2. *Let IFS F be a non-overlapping with attractor A , and let $P_F = \{\pi^{-1}(x) : x \in A\}$, which is a partition of the code space I^∞ . For two non-overlapping IFSs F and G , and fractal transformation T_{FG} , if $P_F = P_G$, then T_{FG} is a homeomorphism.*

2.2. Invariant Measures on the Attractor of an IFS. In this subsection we recall the definition of the invariant measures on an IFS with probabilities, also called p -measures, and determine that the dynamical boundary of the attractor A and a certain subset of A associated with the critical set of A , that we call the inner boundary, have measure zero.

Definition 2.8. Let $p = (p_1, p_2, \dots, p_N)$ satisfy $p_1 + p_2 + \dots + p_N = 1$ and $p_i > 0$ for $i = 1, 2, \dots, N$. Such a positive N -tuple P will be referred to as a **probability vector**. It is well known that there is a unique normalized positive Borel measures μ supported on A and invariant under F in the sense that

$$(2.1) \quad \mu(B) = \sum_{i=1}^N p_i \mu(f_i^{-1}(B))$$

for all Borel subsets B of X . We call μ the **invariant measure of F** corresponding to the probability vector p and refer to it as the **p -measure** (w.r.t. F). To emphasize the dependence on p , we may write μ_p in place of μ .

Example 2.3. This is a continuation of Example 2.1, where $Z = \{I^\infty; s_1, s_2, \dots, s_N\}$. For a probability vector $p = (p_1, p_2, \dots, p_N)$, the corresponding p -measure is the Bernoulli measure ν_p where

$$\nu_p([\sigma_1 \sigma_2 \cdots \sigma_n]) = \prod_{i=1}^n p_{\sigma_i},$$

where $[\sigma_1 \sigma_2 \cdots \sigma_n] := \{\omega \in I^\infty : \omega_i = \sigma_i \text{ for } i = 1, 2, \dots, n\}$ denotes a cylinder set, the collection of which generate the sigma algebra of Borel sets of I^∞ .

The following known result, see for example [15, statement and proof of Theorem 9.3], is relevant to the present work.

Proposition 2.3. *If F consists of similitudes with scaling ratio of f_i equal to $c_i < 1$, and obeys the open set condition, and if the probabilities are chosen such that $p_i = c_i^D$, where D is the Hausdorff dimension of A , then μ_p is equal to the Hausdorff measure on A .*

The Hausdorff measure prescribed in Proposition 2.3 is sometimes referred to as the *uniform measure* on the attractor.

The following result is proved in [17].

Lemma 2.2. *If F is an IFS with probability vector p , corresponding invariant measure μ_p , and Z is the IFS of Example 2.1 with the same probability vector p and corresponding invariant measure ν_p , then*

$$\mu_p(B) = \nu_p(\pi_F^{-1}(B))$$

for all Borel sets B .

The following theorem relates the topological concept of non-overlapping to the p -measures of the dynamical boundary and the inner boundary. It can be viewed as an extension of a result of Bandt and Graf [2], who show that the Hausdorff measure of the critical set of the attractor of an IFS of similitudes in \mathbb{R}^n , that obeys the OSC, is zero.

Theorem 2.1. *Let $F = \{A; f_1, f_2, \dots, f_N\}$ be an IFS (with probabilities p) with attractor A , invariant measure μ_p , dynamical boundary ∂A , and inner boundary \widehat{C} . Let μ_p be an invariant measure for F . If A is non-overlapping then, for all probability vectors p ,*

- (i) $\mu_p(A \setminus \partial A) = 1$;
- (ii) $\mu_p(\widehat{C}) = 0$.

Proof. To simplify notation let p be any probability vector, let $\mu = \mu_p$, and let $v = v_p$, the p -measure on I^∞ introduced in Examples 2.1 and 2.3.

Proof of (i): Let $D \subset I^\infty$ be the set of disjunctive points. If A is non-overlapping then, by Lemma 2.1, $\pi(D) \subset A \setminus \partial A$.

Hence

$$1 \geq \mu(A \setminus \partial A) \geq \mu(\pi(D)) = v(D) = 1,$$

where we have used Lemma 2.2 and the fact that $v(D) = 1$ (for all vectors p), see [25].

Proof of (ii): Let C be the critical set of A . It follows from (1) that $\mu(F^{-1}(C)) = 0$ and therefore $\mu(f_i^{-1}(C)) = 0$ for all i . By the invariance property

$$\mu(C) = \sum_{i=1}^N p_i \mu(f_i^{-1}(C)) = 0.$$

Now, for each j ,

$$\begin{aligned} \mu(f_j(C)) &= \sum_{i=1}^N p_i \mu(f_i^{-1}(f_j(C))) = p_j \mu(C) + \sum_{i \neq j} p_j \mu(f_i^{-1}(f_j(C))) \\ &= \sum_{i \neq j} p_j \mu(f_i^{-1}(f_j(C))) \leq \sum_{i \neq j} p_j \mu(f_i^{-1}(C)) = 0, \end{aligned}$$

the inequality for the following reason: since $f_i^{-1}(S) = f_i^{-1}(f_i(A) \cap S)$, for all $S \subset A$, we have that $f_i^{-1}(f_j(C)) \subset f_i^{-1}(f_i(A) \cap f_j(A)) \subset f_i^{-1}(C)$, and the last equality because $\mu(f_i^{-1}(C)) = 0$. Since this is true for all i , we have $\mu(F(C)) = 0$. Induction can now be used, similarly, to show that $\mu(F^k(C)) = 0$ for all $k \in \mathbb{N}_0$. This suffices to prove (2) in the statement of the theorem. \square

Remark 2.1. By Theorem 2.1, the definition of non-overlapping, i.e., $\partial A \neq A$, is independent of the probability vector p . Also, if an IFS is non-overlapping, then whether or not $\mu_p(C) = 0$ is independent of p . Also, if

$$(2.2) \quad \overline{\bigcup_{k=1}^{\infty} F^{-k}(C)} = \bigcup_{k=1}^{\infty} F^{-k}(C),$$

which occurs for example if A is p.c.f., then the converse to Theorem 2.1 holds, namely, if $\mu_p(C) = 0$ for any probability vector p , then A is non-overlapping. In particular if Equation 2.2 holds, then whether or not $\mu_p(C) = 0$ is independent of the probability vector p .

The proof of the following theorem appears in [21, Theorem 2.1], which also states that, under the assumption of the open set condition (OSC), whether or not $\mu_p(C) = 0$, is independent of p ; but that theorem applies only to an IFS consisting of similitudes.

Theorem 2.2. *Let F be a contractive IFS of similitudes on \mathbb{R}^n , that obeys set condition. If C is the critical set, then $\mu_p(C) = 0$ for all p -measures μ_p (w.r.t. F).*

2.3. Continuity and Measure Preserving Properties of Fractal Transformations. The main results of this subsection are that fractal transformations between non-overlapping attractors are measurable, continuous almost everywhere, and map p -measures to p -measures.

Theorem 2.3. *Let $F = \{A; f_1, f_2, \dots, f_N\}$ be an IFS with non-overlapping attractor A and invariant measure μ . The top section of $\tau : A \rightarrow I^\infty$ is measurable and continuous almost everywhere w.r.t. μ , for all p .*

Proof. We first prove that $\tau : A \rightarrow I^\infty$ is measurable by showing that τ_F is the uniform limit of a sequence of simple functions whose maximal sets upon which τ has constant value are Borel sets. Define the sequence of simple functions $\tau^{(k)} : A \rightarrow I^\infty$ for $k \in \mathbb{N}$ by

$$\tau^{(k)}(x) = \tau(x)|_k \bar{1}$$

for all $x \in A$, where $\bar{1} := 111\cdots$ and $\sigma|_k := \sigma_1 \cdots \sigma_k$. The sequence $\{\tau^{(k)}\}_{k \in \mathbb{N}}$ converges uniformly to τ because $d(\tau^{(k)}(x), \tau(x)) \leq 2^{-k}$; in fact $\tau(x) = \sup\{\tau^{(k)}(x) : k \in \mathbb{N}\}$. To show that τ is measurable, it now suffices to show that the maximal subsets of A on which $\tau^{(k)}(x)$ is constant, namely

$$D_{\sigma_1 \dots \sigma_k} := \{x \in A : \tau^{(k)}(x) = \sigma_1 \dots \sigma_k \bar{1}\},$$

are Borel sets. This is established by showing, by induction, that

$$D_{\sigma_1 \dots \sigma_k} := f_{\sigma_1} \circ f_{\sigma_2} \circ \cdots \circ f_{\sigma_k}(A) \setminus \{f_{\theta_1} \circ f_{\theta_2} \circ \cdots \circ f_{\theta_k}(A) : \theta_1 \dots \theta_k < \sigma_1 \dots \sigma_k\}.$$

That is, the largest set on which $\tau^{(k)}(x)$ is constant is exactly $D_{\pi(x)|_k}$. Each of the sets $f_{\theta_1} \circ f_{\theta_2} \circ \cdots \circ f_{\theta_k}(A)$ is a Borel set, so $D_{\sigma_1 \dots \sigma_k}$ is too.

To prove continuity, let $D = A \setminus \hat{C}$, which is, by Proposition 2.1 is the set of points with exactly one address. Let $x \in D$ and assume, by way of contradiction, that there is a sequence of points $\{x_n\}$ such that $x_n \rightarrow x$, but $\tau(x_n) \not\rightarrow \tau(x)$. Using the notation $\sigma := \tau(x)$ and $\omega_n := \tau(x_n)$, we have $x_n \rightarrow x$, but $\omega_n \not\rightarrow \sigma$. Since code space is compact, by going to a subsequence if needed, we may assume that $\omega_n \rightarrow \omega \neq \sigma$. Now

$$\pi(\sigma) = \pi \circ \tau(x) = x = \lim_{n \rightarrow \infty} x_n = \lim_{n \rightarrow \infty} \pi \circ \tau(x_n) = \lim_{n \rightarrow \infty} \pi(\omega_n) = \pi(\omega),$$

the last equality following from the continuity of the coding map π . This implies that $\omega \neq \sigma$ are both addresses of x , which is a contradiction because $x \in D$ has exactly one address. \square

For an IFS F , let

$$\Gamma_F = \pi_F^{-1}(\hat{C}_F).$$

Consider two non-overlapping IFSs F and G with the same probability vector. With notation as in the Definition 2.7 of fractal transformation, let

$$\begin{aligned} \Gamma_{\{F,G\}} &= \Gamma_F \cup \Gamma_G \\ \Lambda_{\{F,G\}} &= I^\infty \setminus \Gamma_{\{F,G\}} \\ A_F^0 &= \pi_F(\Lambda_{\{F,G\}}) \quad \text{and} \quad A_G^0 = \pi_G(\Lambda_{\{F,G\}}) \\ A_F^1 &= A_F \setminus A_F^0 \quad \text{and} \quad A_G^1 = A_G \setminus A_G^0 \end{aligned}$$

Note that A_F^0 depends also on G and that A_G^0 depends also on F ; similar for A_F^1 and A_G^1 .

Lemma 2.3. *With notation as above*

- (1) $\mu_F(A_F^1) = \mu_G(A_G^1) = 1$,
- (2) *The fractal transformation T_{FG} maps A_F^1 bijectively onto A_G^1 , and maps A_F^0 into A_G^0 .*
- (3) *Restricted to A_F^1 we have $(T_{FG})^{-1} = T_{GF}$; hence $(T_{FG})^{-1} = T_{GF}$ almost everywhere.*

Proof. Using Lemma 2.2 and Theorem 2.1 we have $\mu(\Gamma_F) = \mu(\pi_F^{-1}\hat{C}_F) = \mu_F(\hat{C}_F) = 0$. This implies that $\mu(\Gamma_{\{F,G\}}) = 0$ or $\mu(\Lambda_{\{F,G\}}) = 1$. Again using Lemma 2.2 we have $\mu_F(A_F^1) = \mu_F(\pi_F(\Lambda_{\{F,G\}})) = \mu(\pi_F^{-1}\pi_F(\Lambda_{\{F,G\}})) \geq \mu(\Lambda_{\{F,G\}}) = 1$. This proves statement (1).

Concerning statement (2), by Proposition 2.1, we know that $\pi_F^{-1} = \tau_F$ is single-valued on A_{FG} . Now τ_F takes A_F^1 bijectively onto $\Lambda_{\{F,G\}}$ and π_G takes $\Lambda_{\{F,G\}}$ bijectively onto A_G^1 . Similarly, τ_F takes A_F^0 into $\Gamma_{\{F,G\}}$ and π_G takes $\Gamma_{\{F,G\}}$ into A_G^0 .

Concerning statement (3), restricted to A_{GF} we have $T_{FG} \circ T_{GF} = \pi_G \circ (\tau_F \circ \pi_F) \circ \tau_G = \pi_G \circ \tau_G = I$, the identity. \square

Theorem 2.4. *Assume that both A_F and A_G are non-overlapping, and let μ_F and μ_G be invariant measures associated with the same probability vector. Then*

- (1) $T_{FG} : A_F \rightarrow A_G$ is measurable and continuous a.e. with respect to μ_F ;
- (2) $\mu_F \circ T_{GF} = \mu_G$ and $\mu_G \circ T_{FG} = \mu_F$.

Proof. Since $T_{FG} = \pi_G \circ \tau_F$, statement (1) follows from the continuity of $\pi_G : I^\infty \rightarrow A_G$ and Theorem 2.3.

Concerning statement (2), let B be a Borel set in A_G , and let $B^0 = B \cap A_G^0$, $B^1 = B \cap A_G^1$. By Lemma 2.2 and Lemma 2.3

$$\mu_G(B) = \mu(\pi_G^{-1}B) = \mu(\pi_G^{-1}(B^0 \cup B^1)) = \mu(\pi_G^{-1}B^0) + \mu(\pi_G^{-1}B^1) = \mu(\tau_G B^1),$$

the last equality because $\pi_G^{-1}(B^0) = \tau_G(B^0)$, which has measure zero.

By similar arguments

$$\mu_F(T_{GF}B) = \mu_F(T_{GF}(B^0 \cup B^1)) = \mu_F(T_{GF}B^0) + \mu_F(T_{GF}B^1) = \mu(\pi_F^{-1} \circ \pi_F \circ \tau_G(B^1)) = \mu(\tau_G B^1),$$

the second to last equality because $T_{GF}(B^0) \subset A_F^0$, which has measure zero. \square

3. EXAMPLES OF FRACTAL TRANSFORMATIONS

Example 3.1. (Koch curve)

Let

$$F = \{\mathbb{R}; f_1 = \frac{1}{2} - \frac{x}{2}, f_2 = 1 - \frac{x}{2}\},$$

$$G = \{\mathbb{R}^2; g_1 = (\frac{x}{2} + \frac{y}{2\sqrt{3}} - 1, \frac{x}{2\sqrt{3}} - \frac{y}{2}), g_2 = (\frac{x}{2} - \frac{y}{2\sqrt{3}} + 1, -\frac{x}{2\sqrt{3}} - \frac{y}{2})\}.$$

Then $A_F = [0, 1]$ while A_G is a segment of a Koch snowflake curve. In this case both T_{FG} and T_{GF} are homeomorphisms, because

$$\{\pi_F^{-1}(x) : x \in A_F\} = \{\pi_G^{-1}(x) : x \in A_G\}.$$

Also

$$T_{FG} = T_{GF}^{-1}.$$

If $p_1 = p_2 = 0.5$, then μ_F is uniform Lebesgue measure on $[0, 1]$. The pushforward of μ_F to A_G under T_{FG} is the uniform measure μ_G on A_G that uniquely obeys $\mu_G(\mathcal{B}) = (\mu_G(g_1^{-1}(\mathcal{B})) + \mu_G(g_2^{-1}(\mathcal{B}))) / 2$ for all Borel subsets \mathcal{B} of A_G . (We remark that the measure of any Borel subset \mathcal{B} of A_G may be computed by, and thought of in terms of, the chaos game algorithm on G with equal probabilities, [14].) The Hausdorff dimensions of A_F and A_G are 1 and $2 \ln 2 / \ln 3$, respectively: thus, a fractal transformation may change the dimension of a set upon which it acts.

Example 3.2 (Length preserving fractal transformation of the unit interval). Let $F = \{([0, 1]; f_1, f_2)\}$ and $G = \{([0, 1]; g_1, g_2)\}$, where

$$f_1(x) = rx, \quad f_2(x) = (1-r)x + r$$

$$g_1(x) = rx + (1-r), \quad g_2(x) = (1-r)x,$$

and $0 < r < 1$. The probability vector is $p = (r, 1-r)$, so that the invariant measure for both F and G is Lebesgue measure. By Theorem 2.4, the fractal transformation $T_{FG} : [0, 1] \rightarrow [0, 1]$ preserves length. This example can be generalized from 2 to N functions as long as the scaling factors of f_i and g_i are the same, say r_i , for all i , and the probability vector $p = (p_1, p_2, \dots, p_N)$ satisfies $p_i = r_i$ for all i .

Example 3.3 (Self mappings of the interval). If

$$F = \left\{ \mathbb{R}; f_1 = \frac{x}{2}, f_2 = \frac{x}{2} + \frac{1}{2} \right\},$$

$$G_1 = \left\{ \mathbb{R}; g_1 = -\frac{x}{2} + \frac{1}{2}, g_2 = \frac{x}{2} + \frac{1}{2} \right\},$$

$$G_2 = \left\{ \mathbb{R}; g_1 = -\frac{x}{2} + \frac{1}{2}, g_2 = -\frac{x}{2} + 1 \right\},$$

$$G_3 = \left\{ \mathbb{R}; g_1 = \frac{x}{2}, g_2 = -\frac{x}{2} + 1 \right\},$$

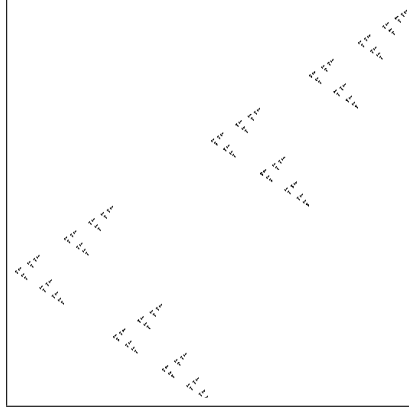


FIGURE 1. Graph of the fractal transformation T_{FG_1} discussed in Example 3.3. This provides a Lebesgue measure-preserving transformation on $[0,1]$ that is continuous a.e. but has a dense countable set of discontinuities. This transformation, and others like it, provide unitary transformations on $\mathcal{L}^2[0,1]$ and "fractal Fourier series", see Section 4. The viewing window is slightly larger than $[0,1] \times [0,1]$.

then $A_F = A_{G_i} = [0,1]$ for $i = 1, 2, 3$. All three fractal transformations T_{FG_i} , $i = 1, 2, 3$, are continuous at all points of $A_F^1 = [0,1] \setminus \widehat{C}$ where \widehat{C} is the diadic set

$$\widehat{C} = \left\{ \frac{k}{2^n} : k = 0, 1, \dots, 2^n; n \in \mathbb{N} \right\}.$$

Indeed, T_{FG_i} , $i = 1, 2, 3$, is a homeomorphism when restricted to $[0,1] \setminus \widehat{C}$. Moreover, T_{FG_i} , $i = 1, 2, 3$, are continuous from the left at all points in $(0,1]$. If we choose $p_1 = p_2 = 0.5$, then the measures $\mu_F = \mu_{G_i}$, $i = 1, 2, 3$, are all the Lebesgue measure on $[0,1]$. The graph of the function T_{FG_1} appears in Figure 1, and the graph of T_{FG_2} appears in Figure 2.

It can be shown by a symmetry argument that T_{FG_2} is its own inverse, i.e., $T_{FG_2} \circ T_{FG_2} = id$, the identity, a.e. This is not obvious from the definition of T_{FG_2} which can be stated by expressing $x \in [0,1]$ in binary representation: if

$$x = \sum_{n=1}^{\infty} d_n/2^n, \quad d_n \in \{0,1\},$$

then

$$T_{FG_2}(x) = \sum_{n=1}^{\infty} (-1)^{n-1} (d_n + 1)/2^n.$$

Example 3.4 (Hilbert's space filling curve). Space filling curves, from the point of view of IFS theory, have been considered in [24]. In [6] it is shown how, as follows, functions such as the Hilbert mapping $h : [0,1] \rightarrow [0,1]^2$ (see Figure 3) are examples of fractal transformations.

Let $A = A_1 = (0,0), B = B_4 = (1,0), C = C_3 = (1,1), D = D_2 = (0,1), B_1 = A_2 = (0,0.5), C_1 = B_2 = A_3 = D_4 = (0.5,0.5), D_1 = C_4 = (0.5,0), C_2 = D_3 = (0.5,1),$ and $B_3 = A_4 = (1,0.5)$. Let

$$F = \left\{ \mathbb{R}; f_i = \frac{x+i-1}{4}, i = 1, 2, 3, 4 \right\},$$

$$G = \{ \mathbb{R}^2; g_i, i = 1, 2, 3, 4 \}$$

where $g_i : \mathbb{R}^2 \rightarrow \mathbb{R}^2$ is the unique affine transformation such that $g_i(ABCD) = A_i B_i C_i D_i$, by which we mean $g_i(A) = A_i, g_i(B) = B_i, g_i(C) = C_i, g_i(D) = D_i$ for $i = 1, 2, 3, 4$. (Similar notation will be used elsewhere in this paper.) The Hilbert mapping is $h = T_{FG} : [0,1] \rightarrow [0,1]^2$. The functions in G were chosen to conform to the orientations of Figure 3, which comes from

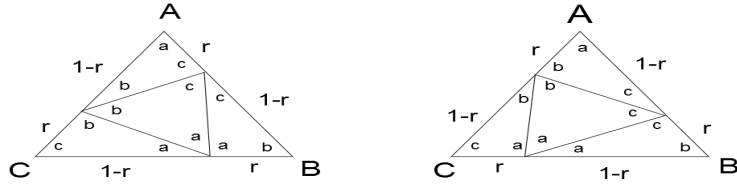


FIGURE 4. See Example 3.6.

the four affine functions as illustrated in the figure on the left, where Δ is mapped to the four smaller triangles so that points A, B, C are mapped, respectively, to points a, b, c . A probability vector is associated with F such that the probability is proportional to the area of the corresponding triangle. The IFS G_λ is defined in exactly the same way, but according to the figure on the right. The attractor of each IFS is Δ . (It is quite a subtle point, that there exists a metric, equivalent to the Euclidean metric on \mathbb{R}^2 , such that both IFSs are contractive, see [?].) It is proved in [11] that the corresponding invariant measures μ_F and μ_G are both 2-dimensional Lebesgue measure. By Theorem 2.4 and [6, Theorem 1], or by [11], the fractal transformation T_{FG}^r is an area-preserving homeomorphism of Δ for all $0 < r \leq \frac{1}{2}$. See [11] for related examples of volume-preserving fractal homeomorphisms between tetrahedra.

4. ISOMETRIES BETWEEN HILBERT SPACES

Given an IFS F with attractor A_F and an invariant measure μ_F , the Hilbert space $L_F^2 = L^2(A_F, \mu_F)$ of complex-valued functions on A_F that are square integrable w.r.t. μ_F are endowed with the inner product $\langle \cdot, \cdot \rangle_F$ defined by

$$\langle \psi_F, \varphi_F \rangle_F = \int_{A_F} \overline{\psi_F} \varphi_F d\mu_F,$$

for all $\psi_F, \varphi_F \in L_F^2$. Functions that are *equivalent*, i.e., equal almost everywhere, will be considered the same function in L_F^2 .

Definition 4.1. Given two IFSs F and G with the same number of functions, with the same probabilities, with attractors A_F and A_G and invariant measures μ_F and μ_G , respectively, let T_{FG} and T_{GF} be the fractal transformations. The **induced isometries** $U_{FG} : L_G^2 \rightarrow L_F^2$ and $U_{GF} : L_F^2 \rightarrow L_G^2$ are given by

$$\begin{aligned} (U_{FG}\varphi_F)(y) &= \varphi_F(T_{GF}(y)) \\ (U_{GF}\varphi_G)(x) &= \varphi_G(T_{FG}(x)) \end{aligned}$$

for all $x \in A_F$ and all $y \in A_G$. That these linear operators are isometries is proved as part of Theorem 4.1 below.

Theorem 4.1. *Under the conditions of Definition 4.1,*

- (1) $U_{FG} : L_G^2 \rightarrow L_F^2$ and $U_{GF} : L_F^2 \rightarrow L_G^2$ are isometries;
- (2) $U_{FG} \circ U_{GF} = id_F$ and $U_{GF} \circ U_{FG} = id_G$, the identity maps on L_F^2 and L_G^2 respectively;
- (3) $\langle \psi_G, U_{FG}\varphi_F \rangle_G = \langle U_{GF}\psi_G, \varphi_F \rangle_F$ for all $\psi_G \in L_G^2$, $\varphi_F \in L_F^2$.

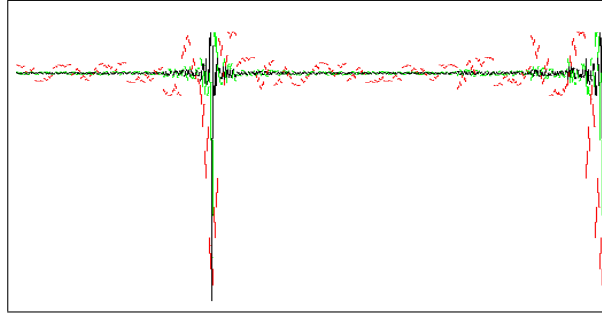


FIGURE 5. Fractal sine series approximations to a constant function on the interval $[0, 1]$. The number of terms used here are 10 (red), 50 (green) and 100 (black). Compare with Figure 6; the r.m.s. errors are the same as for the approximation to the same constant function using a sine series with the same number of terms. Notice that the edge effect has been shifted from 0 to $1/3$.

Proof. (1) To show that the linear operators are isometries:

$$\begin{aligned} \|U_{FG}\varphi_F\|_G^2 &= \int_{A_G} |U_{FG}\varphi_F|^2 d\mu_G \\ &= \int_{A_G} |\varphi_F \circ T_{GF}|^2 d\mu_G \\ &= \int_{A_F} |\varphi_F|^2 d(\mu_G \circ T_{FG}) \\ &= \int_{A_F} |\varphi_F|^2 d\mu_F = \|\varphi_F\|_F^2, \end{aligned}$$

the third equality from the change of variable formula and Lemma 2.3; the fourth equality from statement (2) of Theorem 2.4.

(2) From the definition of the induced isometries

$$(U_{GF} U_{FG}(\varphi_F))(x) = \varphi_F(T_{GF} T_{FG}(x)).$$

But by Lemma 2.3, the fractal transformations T_{GF} and T_{FG} are inverses of each other almost everywhere. Therefore the functions $U_{GF} U_{FG}(\varphi_F)$ and φ_F are equal for almost all $x \in A_F$.

(3) This is an exercise in change of variables, similar to the proof of (1). \square

Example 4.1 (The Cantor function). Consider the two IFS's $F = \{C; \frac{1}{3}x, \frac{1}{3}x + \frac{2}{3}\}$ and $G = \{[0, 1]; \frac{1}{2}x, \frac{1}{2}x + \frac{1}{2}\}$, the first with attractor equal to the standard Cantor set C , the second with attractor equal to the unit interval. In this case the fractal transformation $T_{FG} : C \rightarrow [0, 1]$ is essentially the Cantor function. The Cantor function is usually defined as a function $f : [0, 1] \rightarrow [0, 1]$ so that if x is expressed in ternary notation as $x = i_1 i_2 \dots$ where $i_k \in \{0, 1, 2\}$ for all k , then $f(x) = i'_1 i'_2 \dots$ expressed in binary, where $i' = 0$ if $i \in \{0, 1\}$ and $i' = 1$ if $i = 2$. The function $T_{F,G} : C \rightarrow [0, 1]$ is essentially the same except the domain is C rather than $[0, 1]$.

Let F and G be IFSs with the same probability vectors and corresponding invariant measures μ_F and μ_G . If $\{e_n\}$ is an orthonormal basis for L^2_F , then by Theorem 4.1, the set $\{\widehat{e}_n\} = \{U_{FG} e_n\}$ is an orthonormal basis for L^2_G . In the following example, the two IFSs F and G have the same attractor $A_F = A_G = [0, 1]$, and the invariant measures are both Lebesgue measure. For example, the Fourier orthonormal basis $\{e^{2\pi i n x}\}_{n=-\infty}^\infty$ of $L^2([0, 1])$ is transformed under U_{FG} to a “fractalized” orthonormal basis of $L^2([0, 1])$. Therefore, to any function in $L^2([0, 1])$ there is a Fourier series and also corresponding (via T_{FG}) a fractal Fourier series. (ii) To prove that $U_{FG} U_{GF} = I_F$ we remove from A_F all point that have more than one address w.r.t. F , i.e. those point $x \in A_F$ for which $\pi_F^{-1}(x)$ is not a singleton and we also remove those points of A_F for which $\pi_G^{-1}(T_{FG}(x))$ is not a singleton; this is the set A_F^G defined earlier; it has full measure, and $T_{GF} T_{FG}|_{A_F^G}$ is the identity on A_F^G .

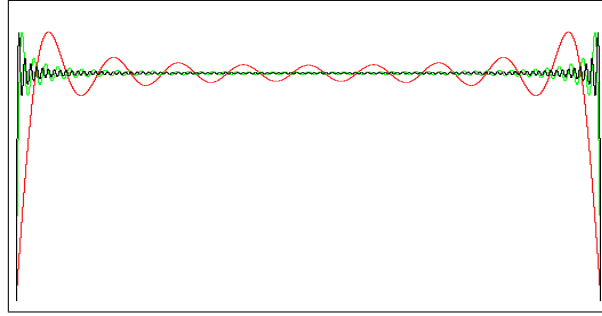


FIGURE 6. For comparison with Figure 5, this shows the Fourier sine series approximations to a constant function on $[0, 1]$ using $k = 10$ (red), 50 (green) and 100 (black) significant terms. Note the well-known end effects at the edges of the interval.

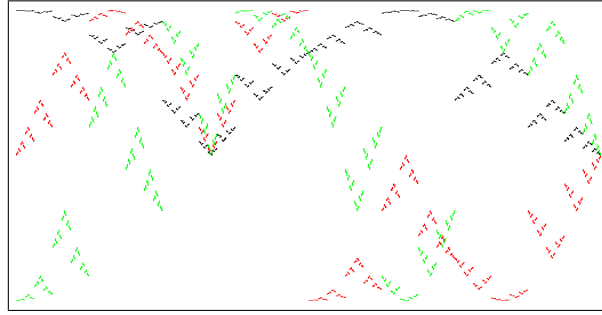


FIGURE 7. See text. The first three eigenfunctions of the elementary fractal transformed Laplacian on $[0, 1]$; equivalently, the functions $f\text{-sin}(n, x)$ for $n=1$ (black), 2 (red), 3 (green). The viewing window is $[0, 1] \times [-1, 1]$.

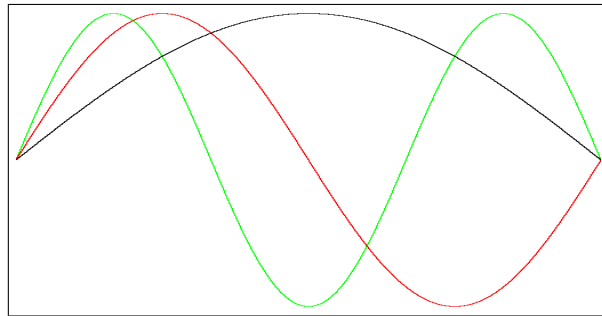


FIGURE 8. This illustrates the sine functions $\sin(n\pi x)$ for $n=1, 2, 3$ for comparison with the fractal sine function shown in Figure 7.

4.1. Fractal Fourier sine series. Consider the IFSs F, G_1, G_2 of Example 3.3 with probabilities $p_1 = p_2 = 0.5$. In this case μ_F, μ_{G_1} and μ_{G_2} are all Lebesgue measure on $[0, 1]$. Consider the orthonormal Fourier sine basis $\{\sqrt{2} e_n\}_{n=1}^{\infty}$ for $L^2[0, 1]$, where $e_n = \sin(n\pi x)$.

For the fractal transformation T_{FG_1} , the fractally transformed orthonormal basis for $L^2[0, 1]$ is $\{\sqrt{2} \hat{e}_n\}_{n=1}^{\infty}$, where

$$\hat{e}_n(x) = \sin(n\pi T_{G_1 F}(x)),$$

for all $n \in \mathbb{N}$. Figure 7 illustrates \hat{e}_i , $i = 1, 2, 3$, in colors black, red, and green, respectively. For comparison, Figure 8 illustrates the corresponding sine functions $\sin(n\pi x)$ for $n = 1, 2, 3$.

Example 4.2 (Constant function). Figure 5 illustrates three fractal Fourier sine series approximations to a constant function on the interval $[0, 1]$, while Figure 6 illustrates the standard sine

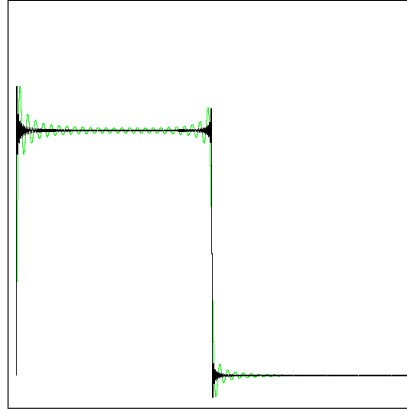


FIGURE 9. Sum of the first 100 (green) and 500 (black) terms in the Fourier sine series for a step function. The viewing window is $[0,1] \times [-0.1,1.5]$. Compare with Figures 10 and 11.

series Fourier approximation using the same numbers of terms. The respective Fourier series are

$$\sum_{n=1}^{\infty} \frac{\widehat{e}_{2n-1}(x)}{2n-1} \quad \text{and} \quad \sum_{n=1}^{\infty} \frac{e_{2n-1}(x)}{2n-1}.$$

The calculation, in the first case, of the Fourier coefficients, uses the change of variables formula, the fact from Example 3.3 that μ_F and μ_{G_1} are Lebesgue measure, and statement 2 of Theorem 2.4. The mean square errors are the same when using the same number of terms.

Example 4.3 (Step function). Next consider Fourier approximants to a step function. The fractal transformation T_{FG_2} has fractal sine functions defined by

$$\widetilde{e}_n := \sin(n\pi T_{G_2 F}(x))$$

for all $n \in \mathbb{N}$. Figures 9, 10, and 11 illustrate the Fourier approximations for 100 (green) and 500 (black) terms, where the orthogonal bases functions are e_n , \widehat{e}_n and \widetilde{e}_n , respectively. The respective Fourier series are

$$\frac{2}{\pi} \sum_{n=1}^{\infty} \frac{1 - \cos(n\pi/2)}{n} f_n(x),$$

where f_n is e_n , \widehat{e}_n and \widetilde{e}_n , respectively. The point to notice is that the jump in the step function at $x = 0.5$ is cleanly approximated in both the fractal series, in contrast to the well-known edge effect (Gibbs phenomenon) in the classical case. The price that is paid is that the fractal approximants have greater pointwise errors at some other values of x in $[0, 1]$. The analysis of where this occurs and proof that the mean square error is the same for all three schemes, is omitted here.

Example 4.4 (Tent function). In Figure 12 partial sums of the Fourier sine series and their fractal counterparts are compared, for the tent function $f(x) = \min\{x, 1-x\}$ on the unit interval. The Fourier series with orthogonal functions e_n is compared with the Fourier series with fractal orthogonal functions \widetilde{e}_n , using 3 (red), 5 (green), 7 (blue), 20 (black) terms. The Fourier series are (up to a normalization constant)

$$\sum_{n=1}^k \frac{2 \sin(\pi n/2) - \sin(\pi n)}{n^2} e_n(x) \quad \text{and} \quad \sum_{n=1}^k \frac{2 \sin(\pi n/2) - \sin(\pi n)}{n^2} \widetilde{e}_n(x).$$

Example 4.5 (Function with a dense set of discontinuities). Consider the following approximation of a function with a dense set of discontinuities. For $i = 1, 2$, let $\psi \in L^2[0, 1]$ be defined by $\psi(x) = x$ for all $x \in [0, 1]$. Then $\phi_i = U_{FG_i} \psi$, $i = 1, 2$, is given by $\phi_i(x) = (U_{FG_i} \psi)(x) = \psi(T_{G_i F}(x)) = T_{G_i F}(x)$, which has a dense set of discontinuities. It follows, by a short calculation using statement 2 of Theorem 2.4, that the coefficients in the \widehat{e}_n and \widetilde{e}_n Fourier series

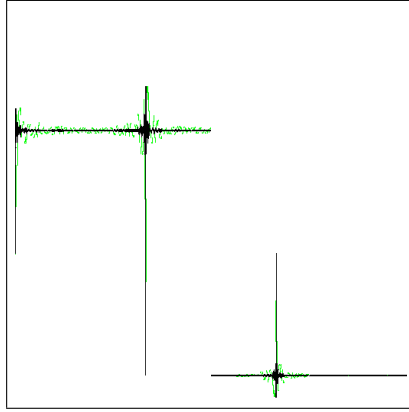


FIGURE 10. Sum of the first 100 (green) and 500 (black) terms in a fractal Fourier sine series (using $f\text{-sin}(n,x)$ functions) for a step function. Compare with Figures 9 and 11.

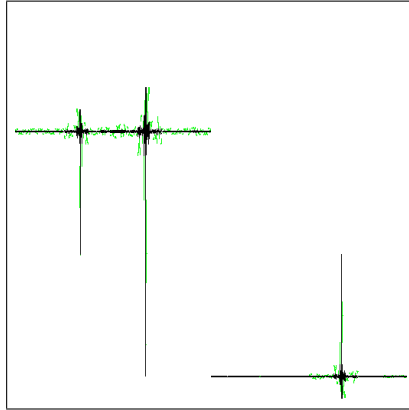


FIGURE 11. Sum of the first 100 (green) and 500 (black) terms in a fractal Fourier sine series (using $f2\text{-sin}(n,x)$ functions) for a step function. Compare with Figures 9 and 10.

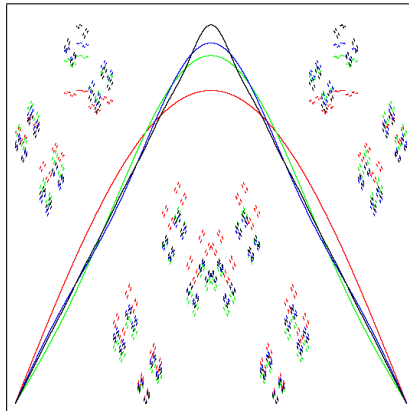


FIGURE 12. See Example 4.4. Fourier sine series approximants to a tent function and fractal counterparts.

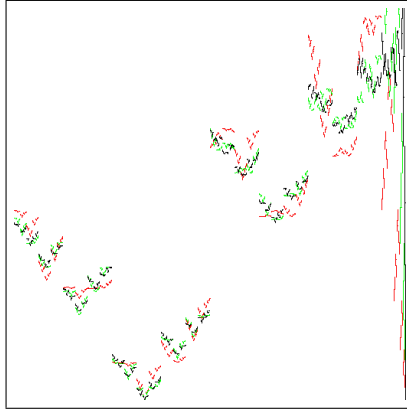


FIGURE 13. See Example 4.5. Compare with Figure 1. The approximants converge to $T_{G_1 F}(x)$ in $\mathcal{L}^2[0, 1]$ as the number of terms in series sum approaches infinity.

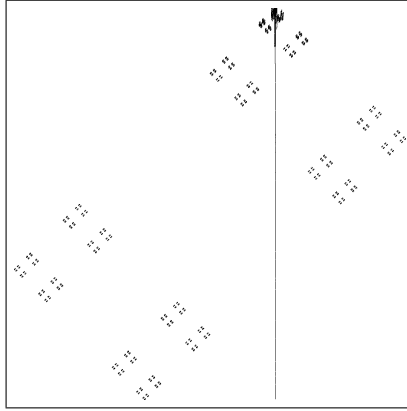


FIGURE 14. See Example 4.5. This illustrates the sum of the first thousand terms of a fractal sine series for $T_{FG_2}(x)$ on $[0, 1]$. Compare with Figure 2.

expansion of ϕ_i are the same as the coefficients in the e_n expansion for ψ . Therefore the fractal version Fourier series expansions for ϕ_i , $i = 1, 2$, are

$$\frac{2}{\pi} \sum_{n=1}^{\infty} \frac{-\cos(\pi n)}{n} \hat{e}_n(x), \quad \text{and} \quad \frac{2}{\pi} \sum_{n=1}^k \frac{-\cos(\pi n)}{n} \tilde{e}_n(x),$$

respectively. Sums with 10, 30, and 100 terms are shown in red, green, and blue, respectively, in Figure 13 for ϕ_1 , and for ϕ_2 in Figure 14 using the first 1000 terms of the series.

4.2. Legendre polynomials. The Legendre polynomials are the result of applying Gram-Schmidt orthogonalization $\{1, x, x^2, \dots\}$, with respect to Lebesgue measure on $[-1, 1]$. Denote the Legendre polynomials shifted to the interval $[0, 1]$ by $\{P_n(x)\}_{n=0}^{\infty}$. They form a complete orthogonal basis for $L^2[0, 1]$, where the inner product is

$$\langle \psi, \varphi \rangle = \int_0^1 \overline{\psi(x)} \varphi(x) dx.$$

In this case each of the unitary transformations U_{FG} associated with Example 3.3 maps $L^2[0, 1]$ to itself, and we obtain the “fractal Legendre polynomials”

$$P_n^{FG}(x) = P_n(T_{GF}(x)).$$

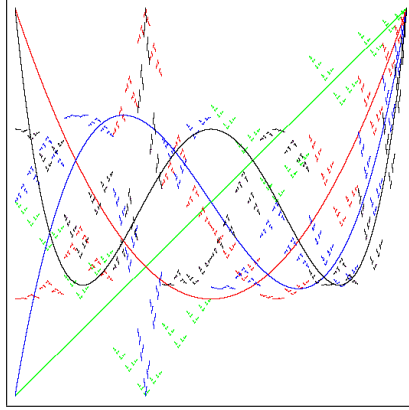


FIGURE 15. Legendre polynomials and their fractal counterparts corresponding to T_{FG_1} . Both sets of functions form orthogonal basis sets with respect to Lebesgue measure on the interval $[-1, 1]$. See also Figure ??.

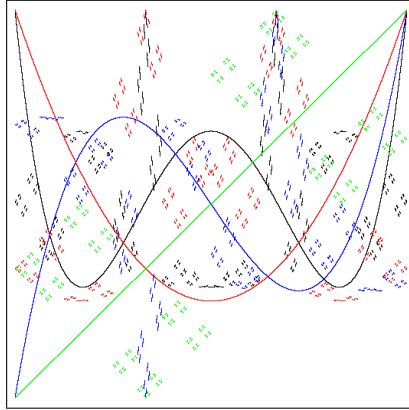


FIGURE 16. Legendre polynomials and their fractal counterparts corresponding to T_{FG_2} . See also Figure 15.

With F, G_1, G_2 as previously defined in Example 3.3, Figures 15 and 16 illustrate the Legendre polynomials and their fractal counterparts. Figure 15 shows the fractal Legendre polynomials $P_n^{FG_1}(x)$ and Figure 16 shows the fractal Legendre polynomials $P_n^{FG_2}(x)$.

4.3. The action of the unitary operator on Haar wavelets. With F, G_2 and $T = T_{FG_2} : [0, 1] \rightarrow [0, 1]$ as previously defined, let $U = U_{FG_2} : L^2[0, 1] \rightarrow L^2[0, 1]$ be the associated (self-adjoint) unitary transformation. Let $I_\emptyset = [0, 1]$ and $H_\emptyset : \mathbb{R} \rightarrow \mathbb{R}$ be the Haar mother wavelet defined by

$$H_\emptyset(x) = \begin{cases} +1 & \text{if } x \in [0, 0.5), \\ -1 & \text{if } x \in [0.5, 1), \\ 0 & \text{otherwise.} \end{cases}$$

For $\sigma \in \{0, 1\}^k$, $k \in \mathbb{N}$, write $\sigma = \sigma_1\sigma_2\dots\sigma_k$ and $|\sigma| = k$. If $|\sigma| = 0$ then $\sigma = \emptyset$, the empty string. Also let $I_\sigma = h_{\sigma_1} \circ h_{\sigma_2} \circ \dots \circ h_{\sigma_k}(I_\emptyset)$, where $h_0 = f_1$ and $h_1 = f_2$, and let $A_\sigma : \mathbb{R} \rightarrow \mathbb{R}$ be the unique affine map such that $A_\sigma(I_\emptyset) = I_\sigma$. With this notation, the **standard Haar basis**, a complete orthonormal basis for $L^2[0, 1]$, is

$$\{H_\sigma : \sigma \in \{0, 1\}^k, k \in \mathbb{N}\} \cup \{H_\emptyset(x)\} \cup \{\mathbf{1}\},$$

where $\mathbf{1}$ is the characteristic function of $[0, 1)$ and $H_\sigma : [0, 1) \rightarrow \mathbb{R}$ is defined by

$$H_\sigma(x) = 2^{|\sigma|/2} H_\emptyset(A_\sigma^{-1}(x)).$$

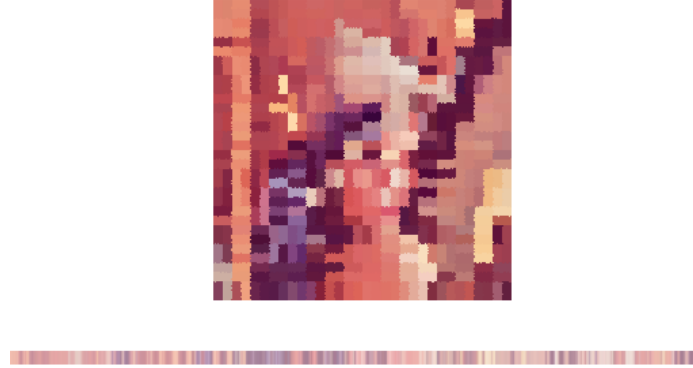


FIGURE 17. See Section 4.4.

There is an interesting action of $U = U_{FG_2}$ on Haar wavelets. The operator U permutes pairs of Haar wavelets at each level and flips signs of those at odd levels, as follows. By calculation, for $\sigma \in \cup_{k \in \mathbb{N}} \{0, 1\}^k$,

$$UH_\sigma = (-1)^{|\sigma|} H_{\sigma'}$$

where $|\sigma| = |\sigma'|$ and $\sigma'_l = (-1)^{l+1} \sigma_l + (1 + (-1)^k)/2$ for all $l = 1, 2, \dots, |\sigma'|$, $UH_\emptyset = H_\emptyset$, and $U1 = 1$. It follows that if $f \in L^2[0, 1]$ is of the special form

$$f = a_\emptyset H_\emptyset + \sum_{\sigma \in \cup_{k \in \mathbb{N}} \{0, 1\}^{2k}} c_\sigma (H_\sigma + H_{\sigma'}),$$

then $Uf = f$ and $f \circ T = f$. Such signals are invariant under U . It also follows that if P is the projection operator that maps $L^2[0, 1]$ onto the span of all Haar wavelets down to a fixed depth, then $U^{-1}PU = P$.

4.4. Unitary transformations from the Hilbert mapping and its inverse. This continues Example 3.4, where the fractal transformations $h := T_{FG}$ and $h^{-1} := T_{GF}$ are the Hilbert mapping and its inverse, both of which both preserve Lebesgue measure and are mappings between one and two dimensions. The unitary transformations $U_{FG} : L^2([0, 1]) \rightarrow L^2([0, 1]^2)$ and $U_{GF} : L^2([0, 1]^2) \rightarrow L^2([0, 1])$ are given by

$$U_{FG}(f) = f \circ h^{-1}, \quad U_{GF}(f) = f \circ h.$$

A *picture* can be considered as a function $f : [0, 1]^2 \rightarrow \mathbb{R}^3$, where the image of a point x in \mathbb{R}^3 gives the RGB colours. The top image of Figure 17 is a picture of the graph of such a function $f : [0, 1]^2 \rightarrow \mathbb{R}^3$. The bottom image is the function (picture) $U_{GF}f = f \circ h$ transformed by the unitary operator.

The Hilbert map $h : [0, 1] \rightarrow [0, 1]^2$ is continuous, one consequence of which is that, if $f : [0, 1]^2 \rightarrow \mathbb{R}^3$ is continuous, then so is the pull-back $U_{GF}(f) = f \circ h : [0, 1] \rightarrow \mathbb{R}^3$. To illustrate, any orthonormal basis w.r.t. Lebesgue measure on $[0, 1]$ is mapped, via the unitary operator U_{FG} , to an orthonormal basis w.r.t. Lebesgue measure on $[0, 1]^2$, and conversely. Because the Hilbert mapping is continuous, an orthonormal basis of continuous functions $\{\psi_n : [0, 1]^2 \rightarrow \mathbb{R}\}$ is transformed by U_{GF} to an orthonormal basis of continuous functions $\{\psi_n \circ h : [0, 1] \rightarrow \mathbb{R}\}$. In the other direction, the image of an orthonormal basis consisting of continuous functions on $[0, 1]$ may not comprise continuous functions on $[0, 1]^2$. Figures 18 and 19 illustrate this.

In Figure 20, the right image represents the graph of $f : [0, 1]^2 \rightarrow [-1, 1]$ defined by $f(x, y) = \sin(\pi x) \sin(\pi y)$. The left image represents the graph of $g : [0, 1]^2 \rightarrow [-1, 1]$ defined by the continuous function $g(x, y) = U_{GF}(f) = f \circ h(x)$ where $h : [0, 1] \rightarrow [0, 1]^2$ is the Hilbert function. The set of functions in the orthogonal basis $\{\sin(n\pi x) \sin(m\pi y) : n, m \in \mathbb{N}\}$ for $L^2([0, 1]^2)$ (w.r.t. Lebesgue two-dimensional measure) is fractally transformed via the Hilbert mapping to an orthogonal basis for $L^2[0, 1]$ (w.r.t. Lebesgue one-dimensional measure). In contrast to the situation in Section 4.1, these "fractal sine functions" are continuous.



FIGURE 18. The bottom band shows the graph of $\sin(\pi x)$ with function values represented by shades of grey. The top band shows the graph of $h(\sin(\pi x))$, where h is the Hilbert function.

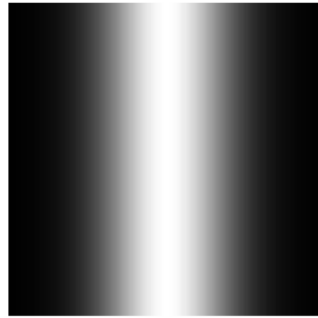


FIGURE 19. The top image illustrates the graph of $f(x, y) = \sin(\pi x)$ for $x, y \in [0, 1]^2$. The band at the bottom illustrates the graph of the pull-back $f \circ h : [0, 1] \rightarrow [-1, 1]$, which is continuous, in contrast to the situations in Figures 17.

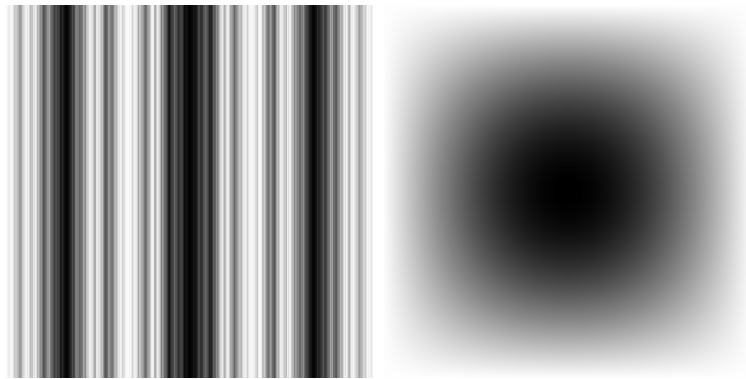


FIGURE 20. The right image represents the graph of $f : [0, 1]^2 \rightarrow [-1, 1]$ defined by $f(x, y) = \sin(\pi x) \sin(\pi y)$. The left image represents the graph of $g : [0, 1]^2 \rightarrow [-1, 1]$ defined by the continuous function $g(x, y) = U_{GF}(f) = f \circ h(x)$ where $h : [0, 1] \rightarrow [0, 1]^2$ is the Hilbert function.

5. FRACTAL TRANSFORMATION OF A LINEAR OPERATOR

Let F and G be IFSs with the same number of functions. Using the same notation as in the previous section, if $W_F : L_F^2 \rightarrow L_F^2$ is a linear operator, then the fractally transformed linear operator $W_G : L_G^2 \rightarrow L_G^2$ defined by

$$W_G = U_{FG} \circ W_F \circ U_{GF}$$

is also a linear operator. If W_F is a bounded, self-adjoint linear operator with spectral representation

$$W_F = \int_{-\infty}^{+\infty} \lambda dP_\lambda^F,$$

where P_λ^F is an increasing family of projections on L_F^2 , then

$$W_G = \int_{-\infty}^{+\infty} \lambda dP_\lambda^G$$

where $P_\lambda^G = U_{FG} \circ P_\lambda^F \circ U_{GF}$. In particular, W_F and W_G have the same spectrum.

5.1. Differentiable functions.

Definition 5.1. Let F and G be IFSs with F and G non-overlapping, and T_{FG} the fractal transformation from A_F to A_G . Assume that the attractor A_F of F is the interval $[0, 1]$, and denote the k times continuously differentiable functions $f : A_F = [0, 1] \rightarrow \mathbb{R}$ by C_F^k . The set

$$C_G^k = \{U_{FG}f : f \in C_F^k\}$$

will be called k **times continuously differentiable fractal functions**. If the k^{th} derivative of $f \in C_F^k$ is denoted $D_F^k f$, where D_F^k is the differential operator, then

$$D_G^k g := (U_{FG} \circ D_F^k \circ U_{GF}) g$$

will be referred to as the k^{th} **fractal derivative of $g \in C_G^k$** .

Note that analogous definitions can be made when A_F is a subset of \mathbb{R}^n with nonempty connected interior, for example a square or filled triangle in the plane. In that case, we have partial derivatives.

To obtain an intuitive interpretation of the fractal derivative, consider the case where the attractor of F (with probability vector p) is $[0, 1]$ as above and F has the property that π_F is an increasing function from the code space to $[0, 1]$ with respect to the lexicographic order on the code space. Assume, similarly, that G (with the same probability vector p) has the property that there is a linear order \preceq on A_G such that π is increasing with respect to this order on A_G and the lexicographic order on the code space. Assume further that T_{FG} is a fractal homeomorphism. Note that all the above assumptions hold in Examples 4.1 of the Cantor set and Example 3.3 of the Koch curve.

For $y_1, y_2 \in A_G$ we use the following notation for the interval: $[y_1, y_2] = \{y : y_1 \preceq y \preceq y_2\}$. Under these assumptions, and with Lebesgue measure μ as the invariant measure of F and μ_G the invariant measure of G , define the **fractal difference** between a pair of points in A_G by

$$y_1 - y_2 = \begin{cases} \mu_G([y_2, y_1]) & \text{if } y_1 \geq y_2, \\ -\mu_G([y_1, y_2]) & \text{if } y_1 < y_2. \end{cases}$$

Theorem 5.1. *With notation as above, if $g : A_G \rightarrow \mathbb{R}$ is a differentiable fractal function, then*

$$D_G g(y_0) = \lim_{y \rightarrow y_0} \frac{g(y) - g(y_0)}{y - y_0}.$$

Proof. If $g : A_G \rightarrow \mathbb{R}$ is a differentiable fractal function, then there is an $f : [0, 1] \rightarrow \mathbb{R}$ such that $g = U_{FG} f$. Now

$$\begin{aligned} D_G g(y_0) &= (U_{FG} \circ \frac{d}{dx} \circ U_{GF} g)(y_0) = ((U_{FG} \circ \frac{d}{dx} \circ U_{GF})(U_{FG} f))(y_0) \\ &= ((U_{FG} \circ \frac{d}{dx}) f)(y_0) = (U_{FG} \circ f')(y) = f'(T_{GF} y_0) = \lim_{x \rightarrow T_{GF} y_0} \frac{f(x) - f(T_{GF} y_0)}{x - T_{GF} y_0}. \end{aligned}$$

Given $x \in [0, 1]$, there is a unique $y_x \in A_G$ such that $T_{GF} y_x = x$. Moreover, since T_{GF} is continuous, as $y \rightarrow y_0$ we have $T_{GF} y \rightarrow T_{GF} y_0$, i.e., $x \rightarrow T_{GF} y_0$. Therefore

$$D_G g(y_0) = \lim_{y \rightarrow y_0} \frac{f(T_{GF} y) - f(T_{GF} y_0)}{T_{GF} y - T_{GF} y_0} = \lim_{y \rightarrow y_0} \frac{g(y) - g(y_0)}{T_{GF} y - T_{GF} y_0}.$$

By Lemma 2.2, if ν is the invariant measure on code space with probability vector p , then (assume $y \succeq y_0$ without loss of generality)

$$\begin{aligned} \mu([T_{GF} y_0, T_{GF} y]) &= \nu([\pi_F^{-1}([T_{GF} y_0, T_{GF} y])]) = \nu([\pi_F^{-1} T_{GF} y_0, \pi_F^{-1} T_{GF} y]) \\ &= \nu([\tau_G y_0, \tau_G y]) = \nu([\pi_G^{-1} y_0, \pi_G^{-1} y]) = \nu(\pi_G^{-1}([y_0, y])) \\ &= \mu_G([y_0, y]) = y - y_0. \end{aligned}$$

Therefore

$$D_G g(y_0) = \lim_{y \rightarrow y_0} \frac{g(y) - g(y_0)}{y - y_0}.$$

□

Example 5.1 (Derivative of the Cantor function). Consider the two IFS's $F = \{[0, 1]; \frac{1}{2}x, \frac{1}{2}x + \frac{1}{2}\}$ and $G = \{\mathcal{C}; \frac{1}{3}x, \frac{1}{3}x + \frac{2}{3}\}$ of Example 4.1. Let $T_{FG} : [0, 1] \rightarrow \mathcal{C}$ be the fractal transformation from the unit interval to the Cantor set. If $f : [0, 1] \rightarrow \mathbb{R}$ is the function $f(x) = x$, for example, then $g := U_{FG} f = T_{GF}$ is exactly the Cantor function described in Example 4.1. The fractal derivative of this Cantor function g is

$$(D_G g)(y) = (U_{FG} \circ D_F \circ U_{GF} g)(y) = (U_{FG} \circ D_F \circ U_{GF} \circ U_{FG} f)(y) = (U_{FG} \circ \mathbf{1}_F)(y) = \mathbf{1}_G(y) = 1$$

for all $y \in \mathcal{C}$, where $\mathbf{1}_F$ and $\mathbf{1}_G$ are the constant 1 functions on $[0, 1]$ and \mathcal{C} , respectively. Therefore the Cantor function has constant a.e. fractal derivative 1.

Since the fractal transformation T_{FG} induces transformations on the set of points of A_F , on the set $L_2(F)$ of functions on A_F , and on the set of linear operators on $L^2(F)$, any differential equation on A_F can be transformed into a differential equation on A_G .

Example 5.2 (Differential equation on the Koch curve). Consider the fractal transformation of Example 3.3, from the unit interval to the Koch curve. The simple initial value ODE

$$\frac{dy}{dx} = y, \quad y(0) = 1$$

on the interval $[0, 1]$ with solution $y = e^x$ transforms to the fractal ODE

$$(U_{FG} \circ \frac{d}{dx} \circ U_{GF}) \hat{y} = \hat{y}, \quad \hat{y}(T_{FG} 0) = 1$$

on the Koch curve. The fractal solution to this ODE is the function $g := U_{FG}(\exp)$, i.e., $g(x) = e^{T_{GF}(x)}$.

6. FRACTAL FLOWS

Let (X, μ) be a metric space with Borel measure μ , and let $f : X \rightarrow X$ be invertible almost everywhere, i.e. if there is a function $f^{-1} : X \rightarrow X$ such that $f \circ f^{-1}(x) = f^{-1} \circ f(x) = x$ for all x in a set of measure 1. Let $\mathcal{M}(X)$ be the set of Borel measures on X . Slightly abusing notation, we use the same symbol $f^\#$ for the following induced actions on $L^2(X)$ and $\mathcal{M}(X)$, respectively:

$$\begin{aligned} f^\#(\phi) &= \phi \circ f^{-1} \quad \text{for } \phi \in L^2(X) \\ f^\#(\mu) &= \mu \circ f^{-1} \quad \text{for } \mu \in \mathcal{M}(X). \end{aligned}$$

Let F be an IFS on the space X , G an IFS on the space Y , and $T_{FG} : X \rightarrow Y$ a fractal transformation. Let μ_F and μ_G be the corresponding invariant measures with respect to the same probability vector. If $f : X \rightarrow X$ is invertible a.e., then define induced actions on $Y, L^2(Y)$,

and $\mathcal{M}(Y)$ as follows. Again we use the same notation $\widehat{f}^\#$ for the induced actions, where $y \in Y, \phi \in L^2(Y)$, and $\mu \in \mathcal{M}(Y)$:

$$\begin{aligned} g(y) &:= \widehat{f}^\#(y) = T_{FG} \circ f \circ T_{GF}(y) \\ \widehat{f}^\#(\phi) &= g^\#(\phi) = U_{FG} \circ f^\# \circ U_{GF}(\phi) \\ \widehat{f}^\#(\mu) &= g^\#(\mu). \end{aligned}$$

Note that, if f is measure preserving on X , then by Theorem 2.4 the induced function g is measure preserving on Y .

By a flow on a space X is meant a mapping $f : X \times \mathbb{R} \rightarrow X$, with notation $f_t(x)$ often used instead of $f(x, t)$, such that

$$\begin{aligned} f_0(x) &= x \\ f_s(f_t(x)) &= f_{s+t}(x) \end{aligned}$$

for all $x \in X$ and all $s, t \in \mathbb{R}$. Applying the induced actions defined above to each function $f_t, t \in \mathbb{R}$, motivates the following notion of fractal flows. Note that there are fractal flows on the metric space Y , and the space of square integrable functions $L^2(Y)$ and on the space of measures $\mathcal{M}(Y)$.

Definition 6.1. A flow f_t on X induces flows $(f_t)^\#$ on $L^2(X)$ and $\mathcal{M}(X)$, and, given a fractal transformation T_{FG} , the flow f_t induces **fractal flows** $(\widehat{f}_t)^\#$ on $Y, L^2(Y)$, and $\mathcal{M}(Y)$. Since, for a flow, $f_t^{-1} = f_{-t}$, the explicit formulas for the flows are

$$\begin{aligned} g_t(y) &:= \widehat{f}_t^\#(y) = T_{FG} \circ f_t \circ T_{GF}(y) \\ \widehat{f}_t^\#(\phi) &= g_t^\#(\phi) = U_{FG} \circ f_t^\# \circ U_{GF}(\phi) \\ \widehat{f}_t^\#(\mu) &= g_t^\#(\mu). \end{aligned}$$

If f_t is a continuous, measure preserving flow on (X, μ) , then it is readily checked that the flow $f_t^\# : L^2(X) \rightarrow L^2(X)$ is unitary, and hence provides a strongly continuous one parameter unitary group. By Stone's theorem [27] there is a unique self-adjoint operator L such that

$$f_t^\# = e^{itL},$$

where iL is referred to as the *infinitesimal generator*. Moreover, $\widehat{f}_t^\# = U_{FG} \circ f_t^\# \circ U_{GF} : L^2(Y) \rightarrow L^2(Y)$ is a fractal flow with infinitesimal generator $i\widehat{L} = U_{FG} \circ L \circ U_{GF}$.

Example 6.1 (Vector field flow). Let $V : \mathbb{R}^2 \rightarrow \mathbb{R}^2$ be a 2-dimensional vector field given by $V(x, y) = (-y, x)$. Define a flow $f : \mathbb{R}^2 \times \mathbb{R} \rightarrow \mathbb{R}^2$, in the usual way by solving the autonomous system

$$\frac{d}{dt} f(\mathbf{a}, t) = V(f(\mathbf{a}, t)), \quad f(\mathbf{a}, 0) = \mathbf{a}.$$

The solution is, with notation $f_t(\mathbf{a}) = f(\mathbf{a}, t)$ and $\mathbf{a} = (a, b)$,

$$f_t(a, b) = (a \cos t + b \sin t, a \sin t - b \cos t).$$

With a, b fixed, as a function of t , the flow curves are circles centered at the origin, so the domain of the flow $f_t(\mathbf{a})$ can be restricted to $D \times \mathbb{R}$, where D is the closed unit disk.

Now consider the area preserving fractal homeomorphism of Example 3.6. Let D be the largest inscribed disk in the equilateral triangle Δ . Without loss of generality, assume that D has radius 1 and consider the flow $f_t(\mathbf{x})$ as in the paragraph above. The fractally transformed flow, as in Definition 6.1, is

$$g_t(\mathbf{y}) = T_{FG} \circ f_t \circ T_{GF}(\mathbf{y}),$$

which as a function of \mathbf{y} , is area preserving. If the fractally transformed vector field is denoted $\widehat{V} = T_{FG} \circ V \circ T_{GF}$, then g_t is the fractal flow of the vector field \widehat{V} . See Figure 21.

Example 6.2 (Fractal flows on the unit interval and the circle). Consider the Lebesgue measure preserving flow on a line segment $[0, 1]$ or the circle S^1 defined by $f_t : [0, 1] \rightarrow [0, 1], t \in (-\infty, \infty)$, defined by

$$x \mapsto (x + t) \bmod 1.$$

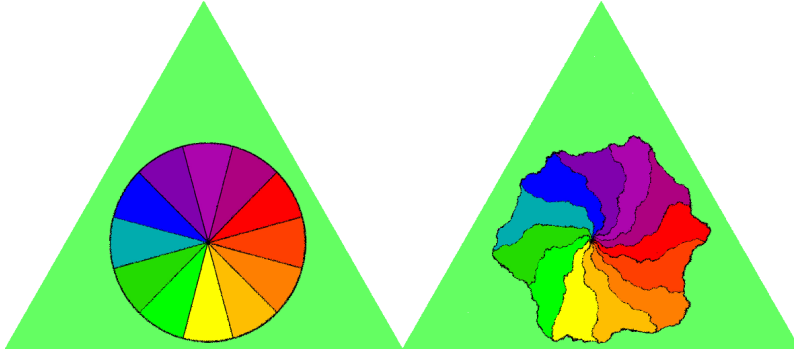


FIGURE 21. This image relates to Example 21.

Consider any measure ρ supported on $[0, 1]$ that is absolutely continuous with respect to Lebesgue measure μ . We may treat ρ as a model for the brightness and colours of a one-dimensional picture: the rate at which light of a set of frequencies is emitted, or reflected, in unit time under steady illumination by the Borel set B is $\rho_0(B)$; see [5]. A vector of measures (ρ_R, ρ_G, ρ_B) represents the red, green, and blue components. With notation as above, $f_t^\# : \mathcal{M} \rightarrow \mathcal{M}$ is a flow on \mathcal{M} . The orbit of a particular measure ρ_0 models the picture being transported/translated at constant velocity along the line segment (what comes out at one end of the line segment immediately reenters the other end) or around the circle S^1 .

Given an initial measure ρ_0 , absolutely continuous with respect to Lebesgue measure, consider its orbit $\rho_t = f_t^\#(\rho_0)$, i.e. $\rho_t(B) = \rho_0(f_{-t}B)$. Interpreted in the model, ρ_t is the translated picture/measure. By the Radon Nikodym theorem there is a measurable function ϱ_0 such that

$$\rho_0(B) = \int_B \varrho_0(x) d\mu = \langle \chi_B, \varrho_0 \rangle$$

for all Borel sets B , where χ_B is the indicator function for B . It follows that

$$\rho_t(B) = \int_B \varrho_t(x) d\mu = \langle \chi_B, \varrho_t \rangle = \langle f_t^\# \chi_B, \varrho_0 \rangle,$$

where $\varrho_t(x) = f_{-t}^\#(\varrho_0)(x) = \varrho_0((x+t) \bmod 1)$, and the last equality by a change of variable. Letting $V_t := f_t^\# : L^2(S^1) \rightarrow L^2(S^1)$, by the comments prior to this example, $f_t^\# = e^{itL}$, where L is a self-adjoint operator. It is well-known that, for this choice of the flow f_t , the operator L is an extension of the differential operator $-i\frac{d}{dx}$ acting on infinitely differentiable functions on S^1 . Therefore, on an appropriate domain,

$$V_t = e^{itL} = e^{t\frac{d}{dx}}.$$

Let $T_{FG} : [0, 1] \rightarrow [0, 1]$ be a uniform Lebesgue measure-preserving fractal transformation, as considered in Section 4.1, and let $U_{FG} : L^2([0, 1]) \rightarrow L^2([0, 1])$ be the corresponding unitary transformation. Then the fractal flow

$$\widehat{V}_t := \widehat{f}_t^\# = U_{FG} V_t U_{GF}$$

is again a strongly continuous one parameter unitary group generated by the self-adjoint operator $\widetilde{L} := U_{FG} L U_{GF}$.

Figure 22 illustrates a fractal flow on $[0, 1]$ for the case of T_{FG_1} in Example 3.3 and Section 4.1. The bottom strip shows an initial function φ on the interval $[0, 1]$. In its orbit $V_t(\varphi)$, $t \geq 0$, this picture slides to the right, colours going off the right-hand end and coming on at the left end, cyclically (not in the figure). From the top of the figure reading downwards, the successive strips show the same orbit under the fractal flow \widehat{V}_t at times $t = 0, 1, 2, \dots, 7$. Then there is a white gap, followed by the flow at time $t = 100$.

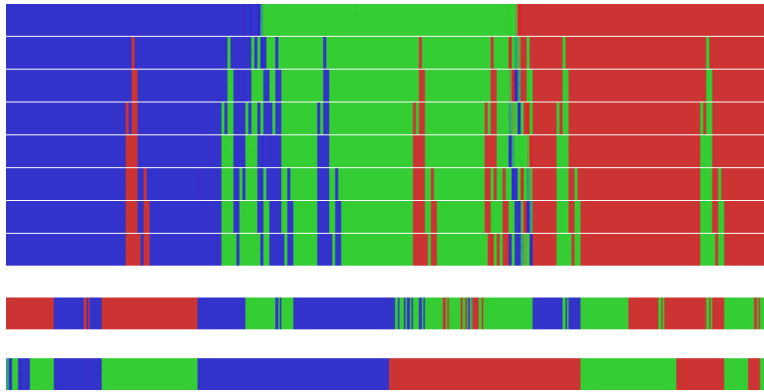


FIGURE 22. See text. Illustration of a fractal flow.

A surprising property of the flow orbit ρ_t is that it is a continuous function of t , although U_{FG} may map continuous functions to discontinuous ones. The proof is a consequence of the fact [26, Proposition 2.5] that $\|f_t^\# \varrho - \varrho\|_{L^1} \rightarrow 0$ as $t \rightarrow 0$.

REFERENCES

- [1] R. Atkins, M. F. Barnsley, A. Vince, D. Wilson, A characterization of hyperbolic affine iterated function systems, *Topology Proceedings* **36** (2010) 189-211.
- [2] C. Bandt, S. Graf, Self-similar sets 7. A characterization of self-similar fractals with positive Hausdorff measure, *Proc. Am. Math. Soc.* **114** (1992) 995-1001.
- [3] M. F. Barnsley, Fractal functions and interpolation, *Constr. Approx.* **2** (1986) 303-329
- [4] M. F. Barnsley, Theory and applications of fractal tops, in *Fractals in Engineering: New Trends in Theory and Applications*, Springer-Verlag (2005) 3-20.
- [5] M. F. Barnsley, *SuperFractals*, Oxford University Press, 2006.
- [6] M. F. Barnsley, Transformations between self-referential sets, *Math. Monthly*, April 2009, 291-304.
- [7] M. F. Barnsley, A. Vince, Fractal tilings from iterated function systems, *Discrete and Computational Geometry*, **51** (2014) 729-752.
- [8] M. F. Barnsley, B. Harding, K. Igudesman, How to transform and filter images using iterated function systems, *SIAM J. Imaging Science*, **4**, 4 (2011), 1001-1028.
- [9] M. F. Barnsley, A. Vince, Fractal homeomorphism for bi-affine iterated function systems, *Int. J. Applied Nonlinear Science*, **1** (2012) 3-19.
- [10] M. F. Barnsley, A. Vince, Developments in fractal geometry, *Bull. Math. Sci.* **3** (2013) 299-348.
- [11] M. F. Barnsley, B. Harding, M. Rypka, Measure preserving fractal homeomorphisms, *Fractals, Wavelets, and their Applications*, C. Bandt et al. (eds.), *Springer Proceedings in Mathematics and Statistics* 92, DOI 10.1007/978-3-319-08105-2_5.
- [12] G. David, S. Semmes, *Fractured Fractals and Broken Dreams: Self-similar Geometry Through Metric and Measure*, Issue 7 of Oxford lecture series in mathematics and its applications, Oxford science publications, Clarendon Press, 1997.
- [13] M. F. Barnsley, A. Vince, Symbolic iterated function systems, fast basins and fractal manifolds, *arXiv:1308.3819v3 [math.DS]* 19 Mar 2014. (A more recent version has been submitted for publication to the *Journal of Fractal Geometry*.)
- [14] J. H. Elton, An ergodic theorem for iterated maps, *Ergodic Theory and Dynam. Systems*, **7** (1987) 481-488.
- [15] K. Falconer, *Fractal Geometry: Mathematical Foundations and Applications*, John Wiley & Sons, 1990.
- [16] D. Hilbert, Über die stetige Abbildung einer Linie auf ein Flächenstück, *Mathematische Annalen*, **38** (1891) 459-460.
- [17] J. Hutchinson, Fractals and self-similarity, *Indiana Univ. Math. J.* **30** (1981) 713-747.
- [18] A. Kameyama, Distances on topological self-similar sets, *Proceedings of Symposia in Pure Mathematics*, **71.1** (2004) 117-129.
- [19] J. Kigami, *Analysis on Fractals*, Cambridge University Press, 2001.
- [20] M. Morán, Dynamical boundary of a self-similar set, *Fundamenta Mathematicae*, **160** (1999) 1-14.
- [21] M. Morán and J. Rey, Singularity of self-similar measures with respect to Hausdorff measures, *Trans. Amer. Math. Soc.*, **350** (1998) 2297-2310.
- [22] J. C. Oxtoby, S. M. Ulam, Measure-preserving homeomorphisms and metrical transitivity, *Annals of Mathematics*, Second Series, Volume 42, Issue 4 (Oct., 1941), 874-920.
- [23] D. Molitor, N. Ott, R. Strichartz, Using Peano curves to construct Laplacians on fractals, *arXiv:1402.2106v1 [Math.FA]* 10 Feb 2014.
- [24] H. Sagan, *Space-Filling Curves*, Universitext, New York, Springer-Verlag, 1994.

- [25] L. Staiger, How large is the set of disjunctive sequences, *Combinatorics, Computability and Logic, Discrete Mathematics and Theoretical Computer Science*, (2001) 215-225.
- [26] E. Stein and R. Shakarchi, *Real Analysis*, Princeton University Press, 2007.
- [27] M. H. Stone, On one-parameter unitary groups in Hilbert space, *Annals of Mathematics* **33** (1932) 643-648.
- [28] R.S. Strichartz, *Differential Equations on Fractals*, Princeton University Press, New Jersey 2006

UNIVERSITY OF GREIFSWALD

AUSTRALIAN NATIONAL UNIVERSITY

AUSTRALIAN NATIONAL UNIVERSITY

AUSTRALIAN NATIONAL UNIVERSITY,